Finite element modeling of guided waves propagation in plates with variable thickness

F. Jenot, M. Ouaftouh, M. Ourak, M. Duquennoy, P. Poussot

Institut d'Electronique de Microélectronique et de Nanotechnologie

Département Opto-Acousto-Electronique (UMR CNRS 8520)

Université de Valenciennes, Le Mont Houy, 59313 Valenciennes cedex 9, France

Abstract: The generation and the detection of acoustic waves by laser sources allow the non-destructive and non-contact testing of many structures and particularly of those having a complex geometry. For example, it is possible to excite simultaneously surface and bulk waves on cylinders of small diameter or on balls of small size.

This type of control often forms part of important industrial issues and in the vast majority of cases, the direct interpretation of the received signals remains difficult. Indeed, various mode conversions can occur following the multiple reflections of waves within the sample. Moreover, it is also possible to observe in certain situations, superposition phenomena which complicate again the analysis of the results. Thus, it appears necessary to have a model able to predict the displacement generated by the waves in a given point of the structure.

In this work, we present numerical results obtained by FEM allowing us to study the propagation of guided waves in plates with linearly variable thickness. A signal processing method which is well suitable to extract the dispersion curves of Lamb modes is first used. Then, the results are analyzed in order to highlight the influence of the thickness variation on the various generated modes. Finally, the A_0 mode dispersion curves are compared with those of structures having a constant thickness and the velocity variations are discussed.

Key words: Laser-ultrasonics, Lamb waves, Thickness, Wavelet transform.

A. Introduction

The use of Lamb waves for the characterization of plates or cylindrical structures is very useful in a great number of practical situations. For example, these guided waves allow the study of corrosion and adhesion phenomena or the detection of cracks [1]-[3]. In the majority of cases, Lamb waves are generated and detected by piezoelectric transducers using the wedge method. Consequently, a contact with the structure and the use of a coupling medium such as oil or water are necessary [4].

In this paper, the propagation of these waves in thin plates with linearly variable thickness is studied. The objective is to quantify, using finite element modeling, the influence of the thickness variation on the dispersion of the Lamb wave modes excited. The considered films have a thickness of the order of a tenth of a millimeter and the fragility of these structures implies naturally the use of a non-contact method of investigation. Laser-Ultrasonics technique which allows the optical generation and detection of acoustic waves in a wide frequency range is thus well adapted to this type of problems [5]-[6]. The present study can find applications in the on-line control of various films particularly during the extrusion process. It can also be seen as a first stage in the characterization of variable thickness coatings for which optical applications are numerous (filters, attenuators).

In a first part, some fundamental properties of Lamb waves are quickly reviewed. Then, the main characteristics of the used model are presented. To finish, the results obtained on a thin aluminum plate are analyzed and discussed.

B. Properties of Lamb waves

Lamb waves are normal modes of vibration of an infinite free elastic plate. The propagation velocities of the various modes depend only on the longitudinal (V_l) and shear (V_t) velocities in the material, as well as on the frequency-thickness product. Figure 1 shows the group and phase velocities of the first two Lamb modes in an aluminum plate ($V_l = 6225$ m/s and $V_t = 3028$ m/s) obtained from numerical resolution of the Rayleigh-Lamb equations [7].
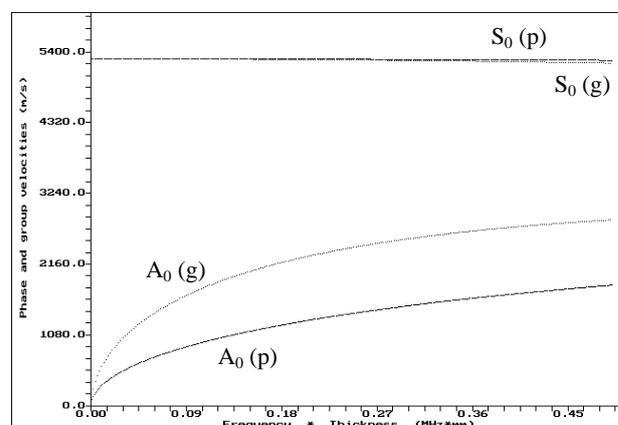
Fig. 1. Phase (p) and group (g) velocities of the first symmetrical (S0) and antisymmetrical (A0) Lamb wave modes for an aluminum plate.

The A_0 and S_0 modes are the only ones to propagate when the frequency-thickness product tends to zero. Using a Mach-Zehnder type of interferometer, the A_0 mode will be better detected than the S_0 mode because it corresponds to a flexion mode and its displacements are essentially normal. For low frequency-thickness products, the propagation velocity of the S_0 mode becomes almost independent of the thickness of the plate and of the frequency. In that case, this velocity is nearly equal to the sheet wave velocity V_p given by the expression:

$$V_p = 2\,V_t \sqrt{1-(V_t/V_l)^2} \tag{1}$$

C. Finite element modeling

The excitation of acoustic waves in a metallic sample using a laser source is based on the conversion of a part of the incident electromagnetic energy into heat. Thus, it is the transient thermal dilation of the material that generates ultrasounds. In thermoelastic mode, when the light power density absorbed does not allow to reach the melting point of the material, a point source located at the sample surface can be modeled (in two dimensions) by a dipole D formed by a pair of tangential forces to this surface. The dipole strength is then given by the expression [5]:

$$D = 3\,\vartheta\,B\,V\,\delta T \tag{2}$$

where ϑ is the coefficient of linear thermal expansion, B the bulk modulus of elasticity, V the volume of matter heated and δT the rise of temperature due to the laser shot. The parameter δT can be easily obtained using the classical heat equation:

$$\nabla^2 T - \frac{1}{\kappa}\frac{\partial T}{\partial t} = -\frac{P_a}{K} \tag{3}$$

where T is the temperature, κ and K correspond respectively to the thermal diffusivity and the thermal conduction of the material and P_a is the light power absorbed by the material per unit of volume [8]. In order to model by finite elements the acoustic waves propagation, it is also necessary to consider the general equation of motion given by the fundamental principle of the dynamics:

$$\overrightarrow{\mathrm{div}\,\overline{\overline{\sigma}}} + \overrightarrow{f_v} = \rho\,\overrightarrow{\gamma} \tag{4}$$

In this expression, $\overline{\overline{\sigma}}$ is the stress tensor, $\overrightarrow{f_v}$ the bulk forces applied to the structure, $\overrightarrow{\gamma}$ the acceleration vector and ρ the density.

It is possible to introduce in the equation (4), the temperature T which is a function of the spatial coordinates and of time. However in that case, the calculus of the displacements in each point of the structure requires the resolution of two coupled equations and the number of nodes is then computationally costly as the time of calculation [9]. An approximate method is to first calculate the rise of temperature at the center of the laser spot and then to assign the temporal dependence of this one to the strengths of the bipolar model presented

previously. Then, the equation (4) allows us to obtain by finite elements the displacements.

D. Geometry of the structure

The structure used in the calculations is presented in figure 2.
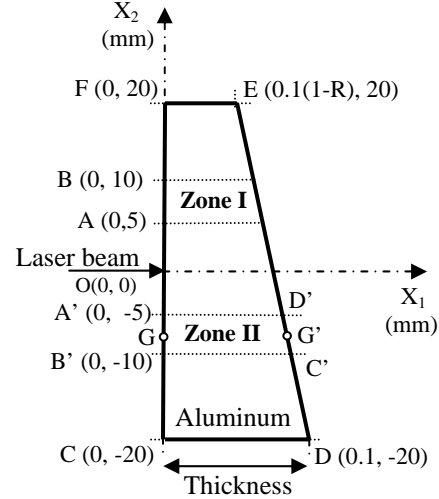
Fig. 2. Schematic of the linearly variable thickness plate studied. R defined the thickness reduction.

The thickness reduction R is defined by the expression:

$$R = 1 - (EF/CD) \tag{5}$$

The length CD is constant in all the simulations and its value is 0.1 mm. The laser beam is located at point O and the normal displacement of the sample surface is calculated at two pairs of points: A, B and A ', B '. Zone I and zone II are respectively defined by the regions of the sample located between each of these pairs of points.

E. Results and discussions

Figures 3(a) and 3(b) present respectively the normal displacement calculated in points B and B ' for R=40 %. These results are obtained using a uniform mesh. The sampling period is 10 ns and the number of nodes is at least 35000 (quadratic elements). These results allow to clearly observe two Lamb modes. At around the time of 2 µs, the S_0 mode is observed with a velocity close to the sheet velocity given by V_p=5291 m/s. This mode is not very sensitive to the variation of thickness because it is slightly dispersive at the frequency-thickness product considered (see Fig. 1). The second wave train represents the A_0 mode whose normal displacement is very large in comparison with the displacement of the S_0 mode. The low frequencies of this mode are very sensitive to the variation of thickness and this independently of the direction of propagation (towards decreasing or increasing thickness). A wavelet transform [10]-[12] of the signals obtained at points A and B as well as at points A' and B' is then computed. It allows to determine the dispersion curve of the A_0 mode and then to evaluate the influence of thickness reduction R on the group velocity. In order to do this, the maximum value of the modulus of

the wavelet coefficients is located in time for each frequency f. It gives us an arrival time noted

$$t_{\alpha_n}(f)$$

where α_n (n=1,2,...) denotes the considered position in space.
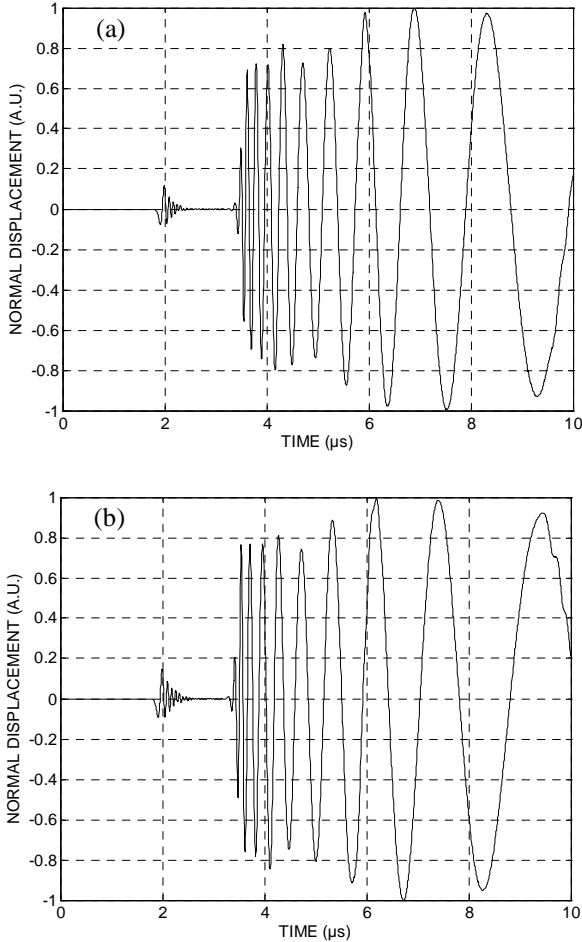
Fig. 3. Normal displacement calculated for a thickness reduction R = 40 % .Figures (a) and (b) correspond respectively to the displacement at point B(0mm, 10mm) and B'(0 mm, -10 mm).

The frequency-dependent group velocity $V_g(f)$ in each zone is then deduced using the expression:

$$V_g(f) = \frac{D}{t_{\alpha_1}(f) - t_{\alpha_2}(f)} \quad (6)$$

where D denotes the distance between A and B also equal to the distance between A' and B'. For zone I, it follows $\alpha_1 = B$, $\alpha_2 = A$ and for zone II, $\alpha_1 = B'$ and $\alpha_2 = A'$.

Results concerning the zones I and II are given respectively in figures 4(a) and 4(b). We note that whatever the zone and the frequency considered, the group velocity decreases with the reduction of thickness. In addition, its evolution according to the frequency seems similar to the dispersion curve of the A_0 mode for a plate of constant thickness with average thickness of the zone considered. The variation of the group velocity according to the thickness reduction R appears more

pronounced in the zone I than in zone II. The first reason is that zone I is more affected than zone II considering their average thickness in comparison with the plate thickness before reduction. The second reason is given by the shape of the A_0 mode dispersion curve. Indeed, for a given frequency, the range of the frequency-thickness product in zone I corresponds to a larger variation of the group velocity than in zone II.
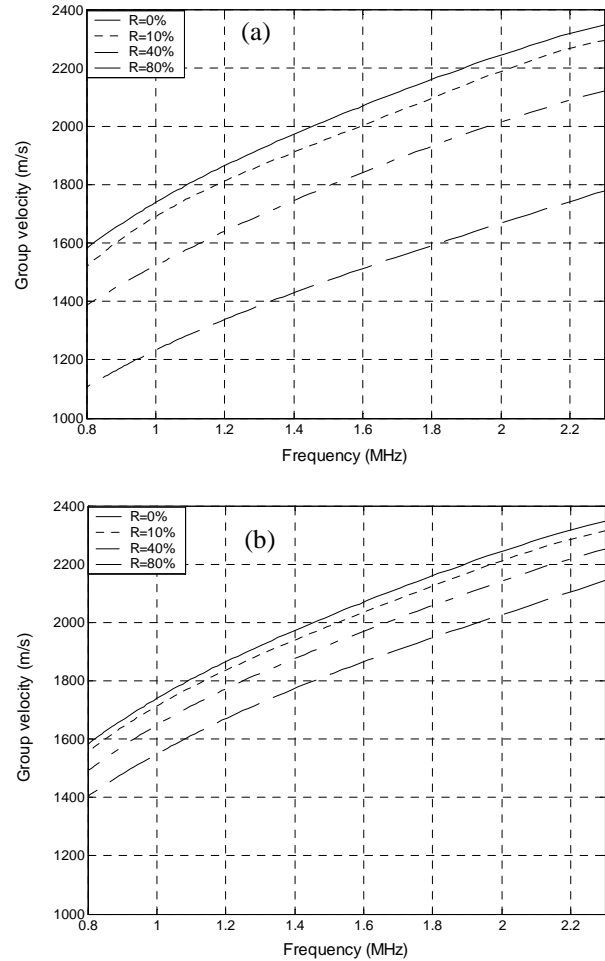
Fig. 4. Influence of the thickness reduction R on the group velocity of the A0 mode. Figures (a) and (b) correspond respectively to the propagation of the wave in zone I and in zone II of the structure.

Thus, each of the previous figures represents a specific chart connected with a zone of the sample. So, this type of chart allows us to deduce the thickness profile of the structure from the group velocity measurement and the knowledge of the length CD. It is also interesting to calculate the dispersion curves of a plate with thickness equal to the average thickness in one of the previous zones for different coefficients of reduction R. In order to do this, zone II is chosen. The average thickness is then given by the distance GG' where G and G' are respectively the middles of the segments [A'B'] and [D'C'] as shown in figure 2. The process to obtain the dispersion curve of the A_0 mode is the same as the one described before in the considered zone. The results are given for different thickness reductions in figure 5. It appears that the dispersion

curves calculated for a variable thickness plate are very close to those calculated for a constant thickness plate. However, when the thickness reduction increases, the difference between these two curves increases too and depends strongly on the frequency range considered.
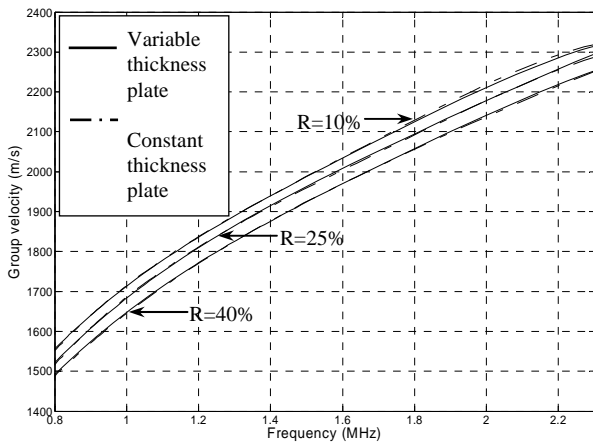
Fig. 5. Dispersion curves of the A0 mode in zone II for variable thickness and constant thickness plates calculated for different thickness reductions R.

This is clearly shown in figure 6 giving the difference of group velocities Vd defined by:

$$V_d = V_{g,v} - V_{g,c} \tag{7}$$

where $V_{g,v}$ and $V_{g,c}$ correspond respectively to the group velocities of plates with linearly variable and constant thickness.
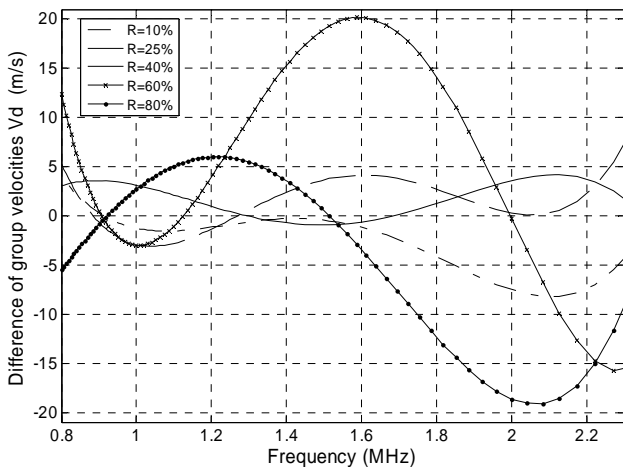
Fig. 6. Difference Vd between the A0 mode group velocities of variable and constant thickness plates in terms of frequency and for different thickness reductions R.

F. Conclusion

In this work, the thermoelastic generation of Lamb waves was considered and their propagation in plates of linearly variable thickness was simulated using a finite element model. It was shown that using the group velocities of the A_0 mode obtained in a specific zone of the sample, it was possible to know the thickness profile of the structure. A comparison of these results with those obtained considering plates of constant thickness was also presented. It has been shown that for thickness reduction up to 40%, the dispersion curves calculated for a specific constant thickness plate are very close to those obtained for a linear variation of plate thickness. Further work is however needed to experimentally confirm these results and to evaluate precisely the accuracy for the thickness measurement.

G. Acknowledgements

H. Literature

[1]   F. Jenot et al., Corrosion thickness gauging in plates using Lamb wave group velocity measurements, Meas. Sci. Technol. 12 (2001), 1287-1293.

[2]   M. J. S. Lowe, P. Cawley, The Applicability of Plate Wave Techniques for the Inspection of Adhesive and Diffusion Bonded Joints, Journal of Nondestructive Evaluation, Vol. 13 No. 4 (1994), 185-199.

[3]   D. N. Alleyne, P. Cawley, The Interaction of Lamb Waves with Defects, IEEE Trans. on Ultra. Ferroel. and Freq. Contr. Vol. 39 No. 3 (1992), 381-397.

[4]   F. Bendec, M. Peretz, S.I. Rokhlin, Ultrasonic Lamb wave method for sizing of spot welds, Ultrasonics March (1984), 78-84.

[5]   C. B. Scruby, L. E. Drain, Laser ultrasonics, Adam Hilger, Bristol, 1990.

[6]   F. Jenot et al., Interferometric detection of acoustic waves at air-solid interface – Applications to non-destructive testing, Journal of Applied Physics, 97, 094905 (2005).

[7]   Viktorov I. A., Rayleigh and Lamb waves, New York:Plenum, 1967.

[8]   D. Royer, E. Dieulesaint, Ondes élastiques dans les solides, tome 2, Masson, Paris, 1999.

[9]   J. H. Lee, C. P. Burger, Finite element modeling of laser generated lamb waves, Computers & Structures Vol. 54 No. 3 (1995), 499-514.

[10] Y. Hayashi et al, Non- contact estimation of thickness and elastic properties of metallic foils by the wavelet transform of laser generated Lamb waves, NDT&E International, 32, (1999), 21-27.

[11] Y. Y. Kim and E. H. Kim, Effectiveness of the continuous wavelet transform in the analysis of some dispersive elastic waves, J. Acoust. Soc. Am., 110 (1), (2001), 86-94.

[12] H. Jeong, Y. S. Jang, Wavelet analysis of plate wave propagation in composite laminates, Composite Structures, 49, (2000), 443-450.